HHS Public Access

Author manuscript

Nature. Author manuscript; available in PMC 2015 March 04.

Published in final edited form as:

Nature. 2014 February 13; 506(7487): 245–248. doi:10.1038/nature12869.

RNA viruses can hijack vertebrate microRNAs to suppress innate immunity

Derek W. Trobaugh[1], **Christina L. Gardner**[1], **Chengqun Sun**[1], **Andrew D. Haddow**[2], **Eryu Wang**[2], **Elik Chapnik**[3], **Alexander Mildner**[4], **Scott C. Weaver**[2], **Kate D. Ryman**[1], and **William B. Klimstra**[1]

[1]Center for Vaccine Research and Department of Microbiology and Molecular Genetics, University of Pittsburgh, Pittsburgh PA, 15261

[2]Institute for Human Infections and Immunity, Center for Biodefense and Emerging Infectious Diseases, and Department of Pathology, University of Texas Medical Branch, Galveston, TX 77555, United States

[3]Department of Molecular Genetics, Weizmann Institute of Science, Rehovot, Israel

[4]Department of Immunology, Weizmann Institute of Science, Rehovot, Israel

Currently, there is little evidence for a significant impact of the vertebrate microRNA (miRNA) system upon the pathogenesis of RNA viruses[1]. This is *primarily* attributed to the ease with which these viruses mutate to disrupt recognition and growth suppression by host miRNAs[2,3]. Here, we report that the hematopoietic cell-specific miRNA, miR-142-3p, potently restricts the replication of the mosquito-borne North American (NA) eastern equine encephalitis virus (EEEV) in myeloid-lineage cells by binding to sites in the 3′ non-translated region (NTR) of its RNA genome. However, by limiting myeloid cell tropism and consequent innate immunity induction, this restriction directly promotes neurologic disease manifestations characteristic of EEEV infection in humans. Furthermore, the region containing the miR-142-3p binding sites is essential for efficient virus infection of mosquito vectors. We propose that RNA viruses can adapt to utilize antiviral properties of vertebrate miRNAs to limit replication in particular cell-types and that this restriction can lead to exacerbation of disease severity.

miRNAs are 21-23 nucleotide host-encoded RNAs that are cell-specific and bind to complementary sequences in the 3′ NTR of host mRNAs[4]. The extent of sequence complementary between the miRNA and mRNA leads to control of mRNA-encoded polypeptide levels by either a block in translation, degradation of the mRNA, or both[5,6]. For

Correspondence and requests for materials should be addressed to W.B.K. (klimstra@pitt.edu).

Supplementary Information is linked to the online version of the paper at www.nature.com/nature.

Author Contributions D.W.T., S.C.W., K.D.R., and W.B.K. designed the experiments and analyzed the data. D.W.T., C.L.G, A.D.H., and E.W. performed the experiments. C.S., E.H., and A.M. provided key reagents. D.W.T and W.B.K. wrote the manuscript. All authors discussed the results and commented on the manuscript.

The authors declare no competing financial interests.

RNA viruses, limited evidence exists for host miRNAs binding to viral RNAs and restricting infection or affecting disease[1,7,8]. In the case of hepatitis C virus (HCV), the opposite is observed: the liver-specific miRNA, miR-122, binds to the viral 5′ NTR, stabilizing the RNA and enhancing *in vitro* viral replication[9,10].

Wild-type (WT) NA EEEV strains are highly virulent mosquito-borne alphaviruses causing a 30-70% case fatality rate in humans[11]. The recognized geographic range and disease incidence of EEEV in the northeastern United States has increased over the past 10 years raising concern about potential widespread outbreaks[12]. EEEV disease is characterized by a limited prodrome prior to manifestations of encephalitis, resulting from restricted myeloid cell replication and minimal induction of systemic type I interferon (IFN)[13,14]. Longer prodromes in human pediatric cases increased the likelihood of recovery, suggesting that host prodromal responses may limit disease severity[15].

WT EEEV is defective for replication in human and murine macrophages and dendritic cells[13]. Using a luciferase-expressing translation reporter RNA encoding the 5′ and 3′ NTRs and translation initiation control sequences of WT EEEV (Extended Data Fig. 1a), we found that translation was restricted in murine RAW 264.7 (RAW) cells, a monocyte/macrophage myeloid cell line, versus BHK-21 fibroblasts (Fig.1a and Extended Data Fig 1d)[13]. Translation of an analogous reporter RNA derived from the related myeloid cell-tropic WT Venezuelan equine encephalitis virus (VEEV) was efficient in both RAW (Fig. 1a) and BHK-21 cells (Extended Data Fig 2a,b)[13,16]. Removal of the EEEV 5′ NTR(EEEV 5′Δ NTR; Extended Data Fig.1b) did not alleviate the restriction in translation in RAW cells (Fig.1a), suggesting the EEEV 3′ NTR confers this restriction. Indeed, transfer of the EEEV 3′ NTR to a host mRNA mimic(5′ host 3′ EEEV; Extended Data Fig. 1c) resulted in translation blockade in RAW cells but not in BHK-21 cells (Fig.1a, and Extended Data Fig 1d). Transfer of the VEEV 3′ NTR to the host mimic had no effect on translation in RAW or BHK-21 cells (Extended Data Fig. 2a, b). Therefore, the EEEV 3′ NTR but not VEEV 3′ NTR contains the restricting element(s).

Two miRNA prediction algorithms, miRANDA[17] and PITA[18], identified three putative canonical and one non-canonical binding sites for the hematopoietic cell-specific miRNA, miR-142-3p, in the 3′ NTR of the NAEEEV strain FL93-939 (Extended Data Fig.3a,b). The three canonical miR-142-3p seed sites are conserved in 17 of 23 sequenced NA EEEV strains collected between 1954 and 2012, suggesting a strong selection for their retention[19] (S. Weaver unpublished data). To determine whether the miR-142-3p binding sites in the EEEV 3′ NTR restrict viral replication, we generated an EEEV mutant (11337) with a deletion of 260 nucleotides encompassing all of the miR-142-3p binding sites (Extended Data Fig.3c). In BHK-21 cells, we observed no significant difference in viral replication at 12 hours post-infection (h.p.i.) with 11337 compared to WT EEEV ($P > 0.2$, Extended Data Fig 3d). However, replication of 11337 in RAW cells (Fig. 1b) was nearly 1000-fold higher than WT EEEV within 8 h.p.i.. A similar phenotype was observed after infection of human K562 and THP-1 monocyte/macrophage cells with WT EEEV and 11337 (Extended Data Fig. 4a, b) as well as primary bone marrow-derived dendritic cells (BMDCs) reported to express high levels of miR-142-3p[20] (Fig. 1c). WT EEEV remained replication-defective in BMDCs in the absence of type I IFN signaling (Extended Data Fig. 4c)[13], however,

replication of 11337 increased, indicating that myeloid cell restriction of WT EEEV is IFN-independent but dependent upon the 3′ NTR sequences containing the miR-142-3p binding sites. All monocyte/macrophage cells used in this study expressed high levels of miR-142-3p in contrast to BHK-21 cells, in which miR-142-3p expression was undetectable (Extended Data Fig. 5).

To confirm a specific role for miR-142-3p in restricting EEEV replication, we expressed miR-142 in BHK-21 cells and assessed its effects on infection by WT EEEV, 11337, and WT VEEV. Ectopic expression of miR-142 in BHK-21 cells (Extended Data Fig. 5) completely blocked WT EEEV infection in comparison to control cells expressing a neuron-specific miRNA, miR-124 (Fig.1d)[21]. In contrast, both 11337 and WT VEEV infected miR-142-expressing BHK-21 cells. To demonstrate the dependence of this restriction on the specific miR-142-3p binding sites, we generated mutant viruses that either had each of the miR-142-3p binding sequences deleted (142del) or three point mutations in each miR-142-3p binding site seed sequence (142pm; Extended Data Fig. 6a,b). These viruses replicated equally well in BHK-21 (Extended Data Fig. 6c) and RAW cells (Fig. 1e) similar to 11337. To confirm the increase in replication in myeloid cells was due to translation of the viral genome, we infected RAW cells with nsP3 reporter viruses to measure translation of virus-particle delivered genomes[13]. Translation was significantly increased by 4 h.p.i. with 142del and 142pm viruses compared to WT EEEV (Fig 1f). Finally, we infected BMDCs derived from miR-142-deficient (miR-142$^{-/-}$) mice[20] with WT EEEV or 11337, and detected no significant difference in viral titers between the viruses after 12 h.p.i.($P > 0.1$, Fig.1g). These data demonstrate that the presence of hematopoietic cell-specific miR-142-3p binding sites in the WT EEEV 3′ NTR results in potent blockade of viral translation and subsequent replication in miR-142-3p-expressing cells *in vitro*.

WT EEEV-infected mice exhibit a minimal prodrome (e.g., ruffled fur, hunched posture, weight loss), which is likely due to restricted myeloid cell replication and minimal type I IFN induction[13, 14]. To assess the contribution of the miR-142-3p binding sites in EEEV to this phenotype, we infected CD-1 mice with WT EEEV and 11337. Survival times were extended in 11337-infected mice compared to WT-infected mice (Fig.2a) with evidence of prodromal disease developing only in 11337-infected mice (Fig.2b). WT EEEV naturally binds heparan sulfate (HS), which limits viral dissemination while also increasing neurovirulence[14]. Therefore, we included a HS binding-defective EEEV mutant (71-77) for a comparison with WT VEEV, which does not bind HS efficiently[14,22]. The 71-77 mutant was significantly attenuated compared to WT EEEV, and elicited signs of prodrome similar to 11337, suggesting that both HS binding and miRNA restriction contribute to the inhibition of prodromal disease. Combining the HS binding-defective mutation with the 11337 deletion (71-77/11337) increased both survival times and prodromal signs compared to WT EEEV or 11337 infection. The timing of prodrome onset following 71-77/11337 infection was only slightly delayed compared to WT VEEV – infected mice (Fig.2b). Consistent with limited prodrome, systemic type I IFN induction is rarely detected during WT EEEV infection (Fig.2c)[13]. However, IFN-α/β was detected by 12 h.p.i. in sera from 11337-infected mice, similar to mice infected with the HS binding mutant 71-77, and both were significantly higher than WT EEEV. Infection with 71-77/11337 elicited higher levels

of IFN-α/β within 8 h.p.i. compared to WT EEEV, and induced at 12 h.p.i., IFN-α/β levels similar to those in sera from WT VEEV-infected mice. These results are consistent with a study in which the addition of artificial miR-142-3p binding sites into the genome of influenza virus reduced IFN-α/β induction in vivo, suggesting that myeloid cell replication may be necessary for serum IFN-α/β induction with multiple viruses[23].

Previously, we observed that serum levels of IFN-α/β and prodromal signs were associated with alphavirus replication in myeloid cells within popliteal lymph nodes (PLN) after footpad inoculation[13, 14]. While WT EEEV replicated poorly in the PLN compared to WT VEEV throughout infection (Fig.2d), both 71-77 and 11337 viruses replicated significantly more than WT EEEV by 12 h.p.i.. The double mutant, 71-77/11337, replicated more efficiently in PLNs at all time points compared to either 71-77 or 11337, and at levels comparable to, but lower than those seen in WT VEEV-infected PLNs. Replication restriction was alleviated for 71-77 and 71-77/11337 in type I IFN receptor-deficient IFNAR1$^{-/-}$ mice (Fig.2d), and survival times for the four viruses were essentially identical ($P > 0.1$; Extended Data Fig. 7) indicating that IFN-α/β is the primary attenuating factor for 11337 and 71-77/11337, and that the 11337 mutation does not compromise replication in vivo in comparison with the WT virus. Fluorescence microscopy and flow cytometric analysis (FCA) of PLNs from mice infected with mCherry-expressing viruses demonstrated the number of cells infected after WT EEEV infection were not significantly different from uninfected mice, but 11337 and 71-77/11337 infected a significantly higher number of cells compared to WT EEEV, with the number of cells infected with 71-77/11337 approaching those seen after WT VEEV infection (Fig. 2e,f). Cells infected by 11337, 71-77/11337 and WT VEEV were predominantly CD11b^{+} with a subset also CD11c^{+} indicative of myeloid lineage cells (Extended Data Fig. 8). 71-77 appeared to infect some PLN cells by microscopy (Fig. 2e), however failure to detect 71-77 PLN infection by FCA (Fig. 2f) is consistent with the presence of miR-142-3p binding sites in the 3′ NTR of this virus. Overall, deletion of the miR-142-3p binding sites alone or in combination with disruption of the HS-binding ability of EEEV increased infection of PLN myeloid-lineage cells, prodromal disease signs, and type I IFN production but decreased virulence in vivo dependent upon a functioning IFN-α/β response.

Given the rapid mutation rate of RNA viruses we hypothesized that the miR-142-3p binding sites in the EEEV 3′ NTR are maintained through positive selection during the mosquito-vertebrate transmission cycle. In C6/36 mosquito cells, the replication of 11337, 142del, and 142pm viruses was significantly reduced compared to WT EEEV at 12 h.p.i (Fig. 3a); however by 24 h.p.i, only the 11337 and 142del viruses remained attenuated. Furthermore, reduced infection rates of the EEEV bridge vector, *Aedes* (*Ochlerotatus) taeniorhynchus*[24], via artificial blood meals were observed for 11337, 142del, and 142pm viruses compared to WT EEEV (Fig. 3b). Therefore, specific sequences of the miR-142-3p binding sites are required for efficient mosquito infection.

We have demonstrated that host miRNA restriction of EEEV replication in myeloid cells is a novel mechanism that determines virus tropism for this cell lineage. Moreover, at least portions of these NTR sequences promote mosquito vector infection, suggesting positive selection as a mechanism for binding site retention during natural EEEV transmission. It is

also clear from these data that, at the organism level, miRNA-mediated restriction of virus replication can lead to suppression of innate immune responses and exacerbation of disease, thereby benefiting the infecting microorganism. Understanding the role of miRNA expression levels and virus genotype in the efficiency of restriction may give insight into temporal, geographical and individual host variation in EEE and potentially other RNA virus diseases.

Materials and Methods Summary

Culture of baby hamster kidney cells (BHK-21), L929 fibroblasts and RAW 264.7 (RAW) monocyte/macrophage cells and bone-marrow derived dendritic cells (BMDCs) from CD-1, IFNAR1$^{-/-}$ and miR-142$^{-/-}$ mice has been described[13,20]. Virus growth curves with BHK-21 cell titration of progeny viruses were performed as described previously[13] using eGFP or mCherry-reporter viruses described below.

WT EEEV, WT VEEV and host mimic luciferase-expressing translation reporters were described previously[25,26]. Other reporters were constructed using the QuikChange II XL mutagenesis kit. Translation assays were performed as described with minor modifications[13].

Construction of cDNA clones of VEEV ZPC 738[27] (WT VEEV), EEEV FL93-939[28] (WT EEEV) and EEEV 71-77[14] were described previously. The EEEV 11337, 142del and 142pm mutants were constructed from the FL93-939 cDNA. mCherry-, eGFP-, and Nano-Luciferase (nLuc)-expressing versions of all viruses were constructed similarly to a described capsid-PE2 fusion reporter viruses using the QuikChange II XL kit[29].

The eGFP-expressing pCMV-miR-142 or pCMV-miR-124, expression plasmids were electroporated into BHK-21 cells. After ∼18 hours, cells were infected with mCherry-reporter viruses for 8 hours followed by assessment of co-expression of the miRNA (eGFP), and virus reporter (mCherry) using fluorescence microscopy.

Outbred CD-1 mice were infected subcutaneously and evaluated for morbidity and mortality as described[13,14]. For tissues, CD-1 or IFNAR1$^{-/-}$ mice were infected with nLuc- or mCherry-reporter viruses. PLNs were harvested at indicated time points and processed for Nano-Glo luciferase assay, for fluorescence microscopy, or for FCA of virus-infected cells. Serum IFN-α/β was measured using a standard biological assay as described[13].

Adult female *A. taeniorhynchus* mosquitoes were infected with EEEV viruses in artificial blood meals. Engorged females were incubated 10 days and assayed for infection by infection of Vero cells and observation for cytopathic effects[30].

Methods

Cell Culture

Baby hamster kidney cells (BHK-21), L929 fibroblasts, and RAW 264.7 (RAW) macrophage-monocyte cells were maintained as described previously[13]. Bone marrow-derived dendritic cells (BMDCs) from CD-1, IFNAR1$^{-/-}$ and miR-142$^{-/-}$ mice[20] were

generated and maintained as previously described[13]. However, miR-142$^{-/-}$ bone marrow was harvested and frozen in 10% DMSO and 90% fetal bovine serum (FBS) prior to culture. *Aedes albopictus* C6/36 mosquito cells were maintained in minimum essential medium alpha medium (Cellgro) supplemented with 10% FBS and 1% L-Glutamine (Gibco).

Translation Reporters and Dual Luciferase Assay

WT EEEV, WT VEEV and host mimic luciferase-expressing translation reporters (diagram in Extended Data Fig. 1) were generated previously[25,26]. The host mimic translation reporters encode a short 5′ and 3′ NTR fused in frame with the fLuc gene. The EEEV 5′Δ NTR and VEEV 5′Δ NTR reporters were constructed using QuikChange II XL mutagenesis kit (Agilent Technologies, Santa Clara, CA) and the primers listed in Extended Data Table 1. The chimeric 5′ host 3′ EEEV and 5′ host 3′ VEEV translation reporter was constructed by addition of a restriction endonucleases site into the host fLuc mimic reporter using QuikChange II XL mutagenesis and the primers listed in Extended Data Table 1. The 3′ NTR of EEEV or VEEV was then placed into the host fLuc mimic after the fLuc gene with endonuclease digestion. Translation assays were performed as described previously with modifications[13]. Each *in vitro* transcribed reporter RNA (7.5 μg/reaction) and the Renilla reporter RNA (0.75 μg/reaction) were electroporated into RAW and BHK-21 cells (6×10^6 cells/reaction) using the Neon Transfection system (Invitrogen; BHK-21: 1200 V, 30 ms, 1 pulse. RAW: 1750 V, 25 ms, 1 pulse). Two reactions were combined and aliquoted in triplicate per time point per experiment. Firefly relative light units (RLU) data were normalized to Renilla RLUs in each sample.

Viruses

Construction of cDNA clones of VEEV ZPC 738[27] (WT VEEV), EEEV FL93-939[28] (WT EEEV) and EEEV 71-77[14] were previously described. mCherry, eGFP, and Nano-Luciferase (nLuc) reporter viruses were constructed as a cleavable in-frame fusion between the capsid and E3 proteins using QuikChange II XL mutagenesis kit with the first 5 amino acids of E3 fused in-frame to the amino terminus of the reporter genes and the 2A-like protease of *Thosea asigna* virus (TaV) fused to the carboxy terminus (C.S., C.L.G., K.D.R. W.B.K. manuscript in preparation)[29]. The EEEV 11337, 142del and 142pm mutants were generated using the EEEV FL93-939 cDNA clone and QuikChange mutagenesis II XL kit and primers listed in Extended Data Table 2. WT EEEV nsP3-nLuc translation reporter virus was constructed with the nLuc gene fused in frame with nsP3 (C.S., C.L.G., K.D.R. W.B.K. manuscript in preparation)[13]. The 3′ NTR of each mutant was placed into TaV and nsP3-nLuc reporter viruses using EcoRI and Not I.

Virus Infections and Plaque Assay

Virus growth curves were performed as described previously using eGFP or mCherry reporter viruses described above[13]. Briefly, BHK-21, RAW and C6/36 cells (2×10^5 cells/well) were infected in triplicate in 24 well plates at a multiplicity of infection (MOI) of 0.1 plaque forming units (PFU)/cell or 1 PFU/cell(C6/36). BMDCs (1×10^5 cells) were infected in triplicate at an MOI of 5 PFU/cell in suspension, washed and transferred into 24 well plates. For growth curves, supernatant was harvested at time zero and indicated time points

for titration by plaque assay on BHK-21 cells. For nsP3 translation reporter assays, RAW (4×10^5 cells/well) were infected at an MOI of 1 PFU/cell in triplicate with nsP3-nLuc reporter viruses and harvested at indicated time points using 1× Passive Lysis Buffer (PLB; Promega). nLuc expression was quantified using the Nano-Glo Luciferase assay system (Promega) according to manufacturer's guidelines and normalized to protein concentration using a Pierce BCA protein assay (Thermo Scientific, Rockford, IL).

miRNA overexpression

The pCMV-miR-142 expression plasmid and a neuron-specific miRNA, pCMV-miR-124, (OriGene, Rockville, MD) were electroporated (4 μg each) into BHK-21 cells (1×10^6 cells) using the Amaxa Nucelofector Kit L (Lonza, Basel, Switzerland) according to manufacturers guidelines. After ∼18 hours, cells were infected with WT EEEV, WT VEEV or EEEV 11337 mCherry TaV viruses (MOI = 1 PFU/cell) for 8 hours followed by fixation. Co-expression of the miRNA (eGFP), and virus reporter (mCherry) was determined using fluorescence microscopy as previously described[13]. Data is represented as the ratio of the percentage of cells co-expressing the microRNA, miR-142, (eGFP) and virus-infected (mCherry) to cells co-expressing miR-124 and virus-infected.

RT-PCR to detect miR-142-3p

Total cellular RNA was harvested from cells using Trizol (Life Technologies) and 1-bromo-3-chloropropane (BCP) and isopropanol. RNA (200 ng) was reverse transcribed with the miScript II RT kit (Qiagen, Germantown MD) according to manufacturers' guidelines. cDNA was diluted in water and mature miR-142-3p was quantified using the miScript SYBR Green PCR kit (Qiagen) according to manufacturers' guidelines using the miR-142-3p specific primer 5′-TGTAGTGTTTCCTACTTTATGGA-3′. miR-142-3p expression was normalized to RNU6B using the primer 5′-GATGACACGCAAATTCGTGAA-3′ and the $\Delta\Delta C_T$ method. Data is calculated as fold change in expression compared to expression of miR-142-3p in BHK-21 cells in which miR-142-3p expression was undetected.

Mouse infections, Tissue Harvest, nLuc Analysis

Six-week old female outbred CD-1 mice (Charles River Laboratories) and 6-9 week old female or male IFNAR1$^{-/-}$ mice bred in house were randomly distributed, infected subcutaneously (sc) in both footpads and scored daily for clinical signs and weight loss as described previously[13, 14]. Two investigators were used to analyze the clinical symptoms observed in the mice during morbidity and mortality studies. Investigators were not privy to timing and onset of clinical symptoms from previous experiment. For tissue harvest, mice were infected with 10^3 PFU of nLuc- or mCherry-reporter TaV viruses. Popliteal lymph nodes (PLN) were harvested at indicated time points and either frozen on dry ice, placed in 200 μl 1× PLB for nLuc analysis or placed in 4% paraformaldehyde (PFA) for one week for visualization on a fluorescence microscope. PLN were homogenized and analyzed for nLuc expression using the Nano-Glo Luciferase assay system. All EEEV PLN were photographed using equal exposure times (615 ms) while the VEEV LN, due to an increased signal, was visualized using a lower exposure time (90 ms) at 4× magnification using cellSens Standard software (Olympus). The 71-77/11337 inset was imaged at 40× magnification and 457 ms

exposure length. Brightness and contrast of the images were adjusted equally using Adobe Photoshop CS3 and Microsoft Powerpoint software. All animal procedures were carried out in accordance with American Association for the Accreditation of Laboratory Animal Care International-approved institutional guidelines for animal care and use and approved by the University of Pittsburgh Institutional Animal Care and Use Committee. No statistical methods were used to ensure adequate power. Sample sizes were chosen based upon experience with the mortality kinetics of EEEV in mice and historical group number requirements to achieve statistical significance yet utilize the fewest animals possible.

Quantification of virus-infected cells from PLN

To quantify number of virus infected cells in PLN, CD-1 mice were infected as above, and PLNs were harvested 12 h.p.i., minced, and incubated with Liberase TL (0.2 mg/ml; Roche) and DNaseI (0.2 mg/ml; Roche) for 20 min at 37°C. After removal of cellular debris, cells were stained with anti-mouse CD16/32 (93; eBioscience), and Fixable Viability Dye eFluor 506 (eBioscience). After washing, cells were stained with anti-mouse CD11b (clone N418, Tonbo Biosciences, San Diego, CA), and anti-mouse CD11c (M1/70; eBioscience) to identify myeloid cells. Cells were fixed in 4% PFA and analyzed using a BD LSRFortessa (BD Bioscience) and FloJo Software (Tree Star Inc., Ashland, OR). Number of virus-infected cells was calculated based on total number of cells in both PLNs per mouse.

IFN-α/β Analysis

Serum IFN-α/β was measured using a standard biological assay on L929 cells as described previously[13].

Mosquito Infection

Adult female *Aedes (Ochlerotatus) taeniorhynchus* mosquitoes were infected with EEEV, 11337, 142del and 142pm mCherry- or eGFP-reporter TaV viruses in artificial bloodmeals. Engorged females were incubated at 27°C for 10 days under 12 hour light/12 hour dark circadian lighting conditions and assayed for infection by inoculation onto Vero cell monolayers and observation for cytopathic effects as described previously[30].

Statistical Analysis

Statistical significance for mortality curves was determined by Mantel-Cox log-rank test. For all viral growth curve experiments, data was $\log_{10}$ transformed and unpaired t tests were performed and corrected for multiple comparisons using the Holm-Sidak method with an alpha = 0.05. For all other experiments, a two-tailed unpaired t test was used (GraphPad Prism software). Statistical analysis for nLuc expression in CD-1 PLN was performed comparing WT EEEV versus the other EEE viruses while WT VEEV was compared to only 71-77/11337 at each time point. nLuc expression in IFNAR1$^{-/-}$ mice was compared to the corresponding viruses at 12 h.p.i. in CD-1 mice only. Statistical analysis for quantification of the number of infected cells in PLN was performed between the EEEV mutant viruses and WT EEEV, and between WT VEEV and 71-77/11337.

Extended Data

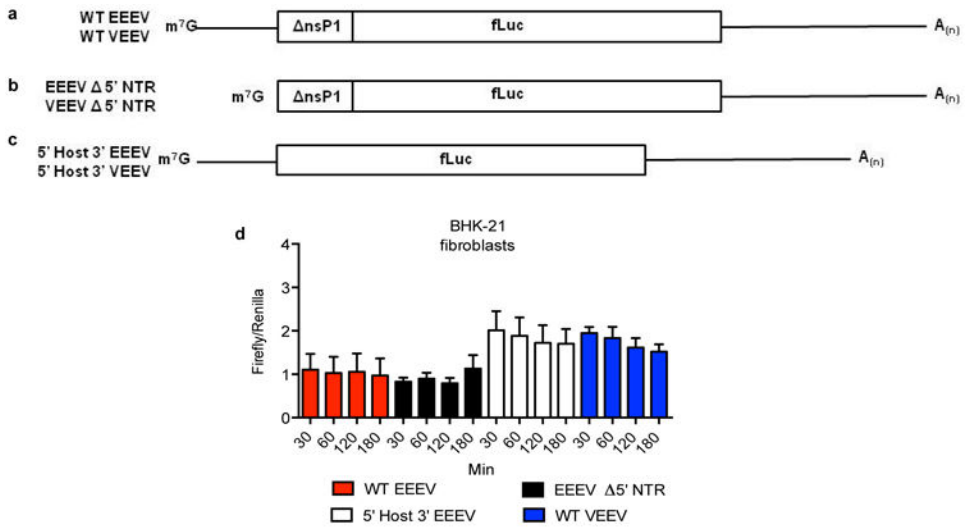

Extended Data Figure 1. EEEV 3′ NTR does not restrict translation in BHK-21 fibroblasts

a. WT EEEV and WT VEEV translation reporters encode the translational initiation control sequences fused to the fLuc gene. **b.** The EEEV 5′ Δ NTR and VEEV 5′ Δ NTR encode the truncated nsP1 gene and only the 3′ NTR of either EEEV or VEEV. **c.** The 3′ NTR of EEEV or VEEV was inserted into a host mRNA mimic reporter to generate the 5′ host 3′ EEEV or 5′ host 3′ VEEV reporters. All translation reporters contain a 5′ cap and a 3′ poly (A) tail. **d.** Translation of WT EEEV, EEEV 5′ Δ NTR, and 5′ host 3′ EEEV reporters in BHK-21 cells. Error bars represent mean ± S.D. and the data are averaged from three independent experiments performed in triplicate.

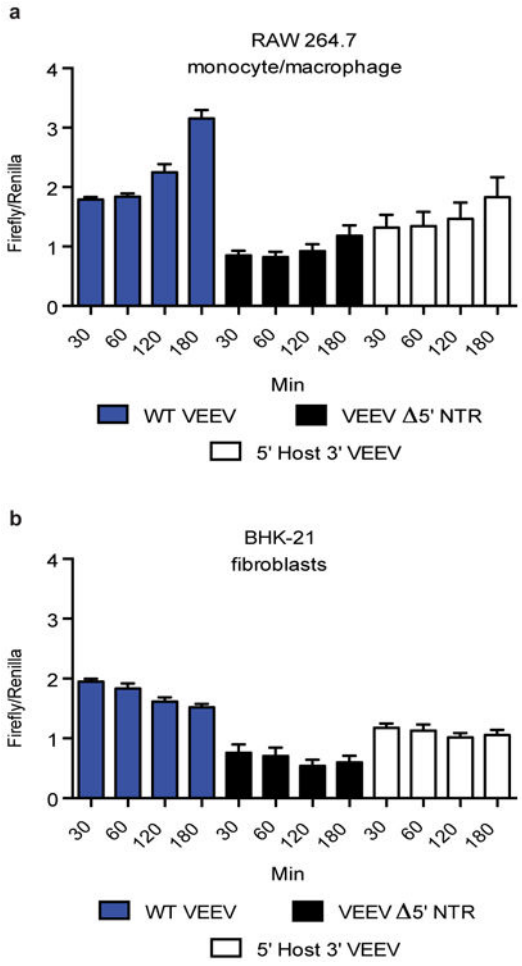

Extended Data Figure 2. VEEV 3′ NTR does not restrict translation in myeloid cells

Translation of WT VEEV, VEEV 5′ Δ NTR, and 5′ host 3′ VEEV reporters in RAW (**a**) and BHK-21 (**b**) cells. Error bars represent mean ± S.D. and the data are averaged from three independent experiments performed in triplicate.

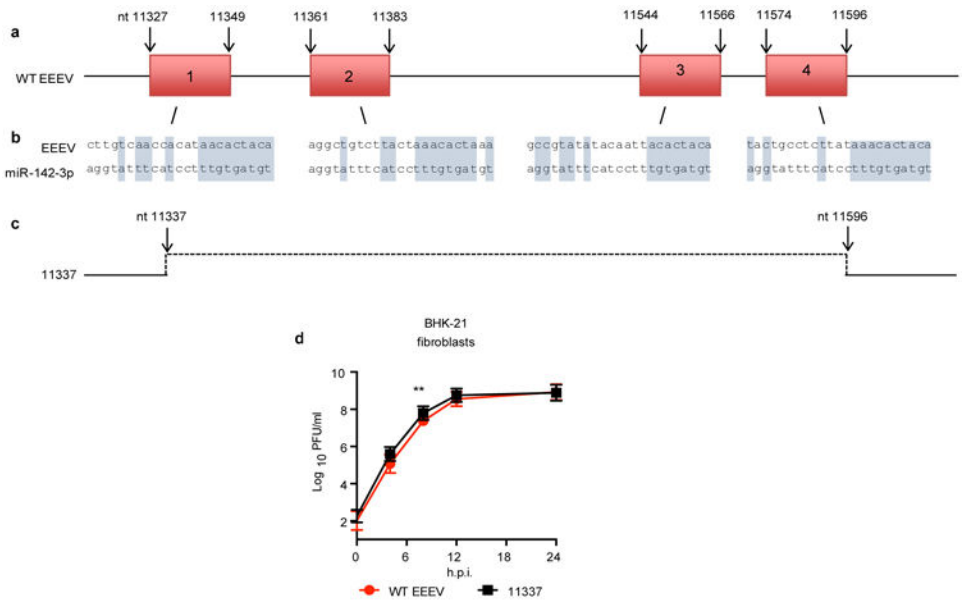

Extended Data Figure 3. Removal of miR-142-3p binding sites in the 3′NTR of EEEV does not alter replication in BHK-21 fibroblasts

a. Red boxes indicate the four miR-142-3p binding sites in the 3′ NTR. Numbers represent nucleotide (nt) positions at the start and end of each miRNA binding site. **b.** Gray boxes correspond to the complimentary nts in the EEEV 3′ NTR and miR-142-3p. **c.** EEEV mutant 11337 contains a deletion in the 3′ NTR from nt 11337 to 11596. **d.** Replication of WT EEEV and 11337 in BHK-21 cells. *n* = 3 independent experiments. Error bars indicate geometric mean ± S.D., and asterisks indicate differences that are statistically significant (**p<0.01).

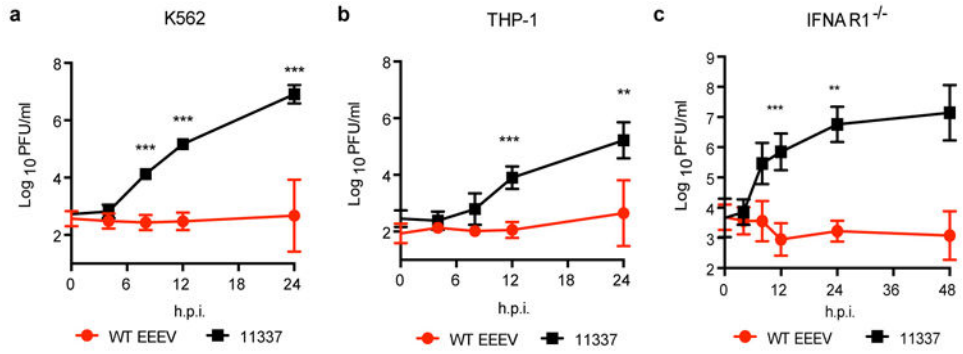

Extended Data Figure 4. miR-142-3p binding sites in EEEV restrict replication in human macrophage/monocyte cell lines and primary murine IFNAR$^{-/-}$ BMDCs

a-b. Replication of WT EEEV and 11337 in human K562 (**a**) and THP-1 (**b**) cells. *n* = 2 (THP-1) and 3 (K562) independent experiments. **c**. Removal of type I IFN does not alleviate WT EEEV restriction in primary murine IFNAR$^{-/-}$ BMDCs. *n* = three independent experiments. Data represent the geometric mean ± S.D., and asterisks indicate differences that are statistically significant (*p < 0.05, **p < 0.01, ***p < 0.001).

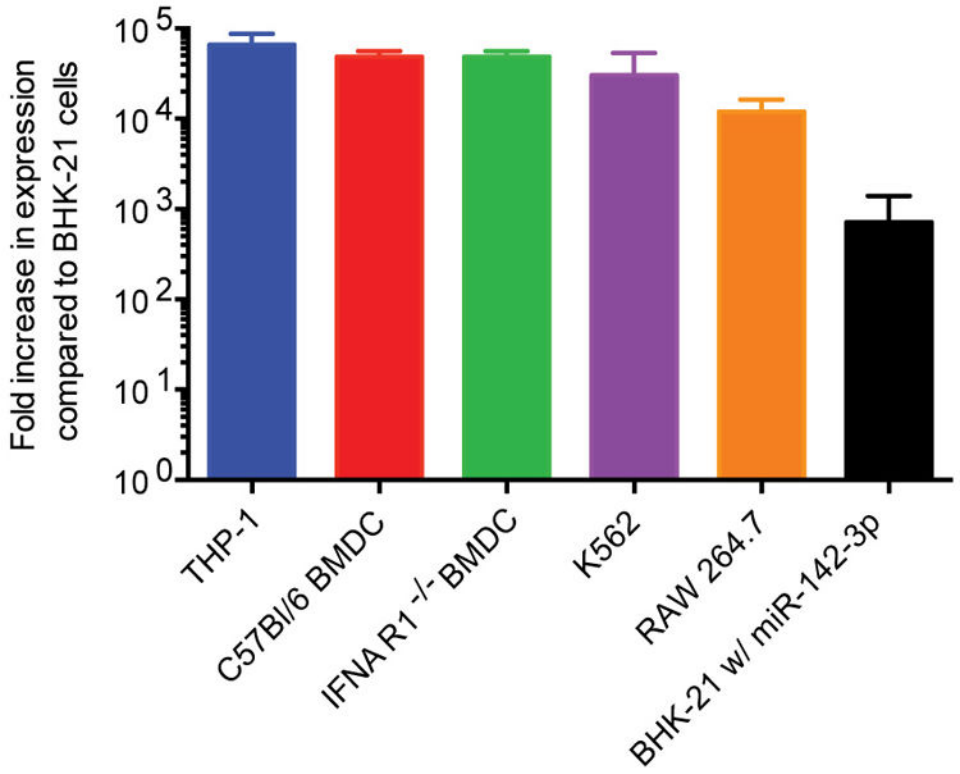

Extended Data Figure 5. Relative expression of miR-142-3p in mouse and human cells

Quantitative RT-PCR on primary murine BMDCs, murine and human monocyte/macrophage cell lines, and BHK-21 cells expressing miR-142-3p (BHK-21 w/miR-142-3p). Fold increase in expression is calculated compared to expression of miR-142-3p in BHK-21 cells in which miR-142-3p expression was undetectable.

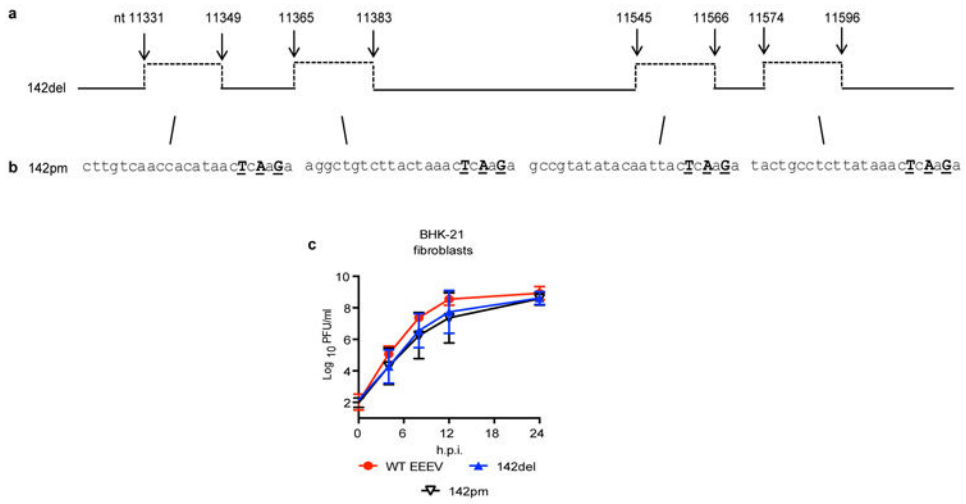

Extended Data Figure 6. Specific deletion of the miR-142-3p binding sites in the 3′ NTR of WT EEEV does not alter replication in BHK-21 fibroblasts

a. EEEV 142del virus contains four deletions corresponding to the complimentary nucleotides in the 3′ NTR that bind to miR-142-3p eliminating all four miR-142-3p binding

sites. **b.** EEEV 142pm virus contains three point mutations in each of the miR-142-3p binding sites that correspond to the seed sequence of miR-142-3p. **c.** Replication of WT EEEV and 11337 in BHK-21 cells. *n* = three independent experiments. Error bars indicate geometric mean ± S.D.

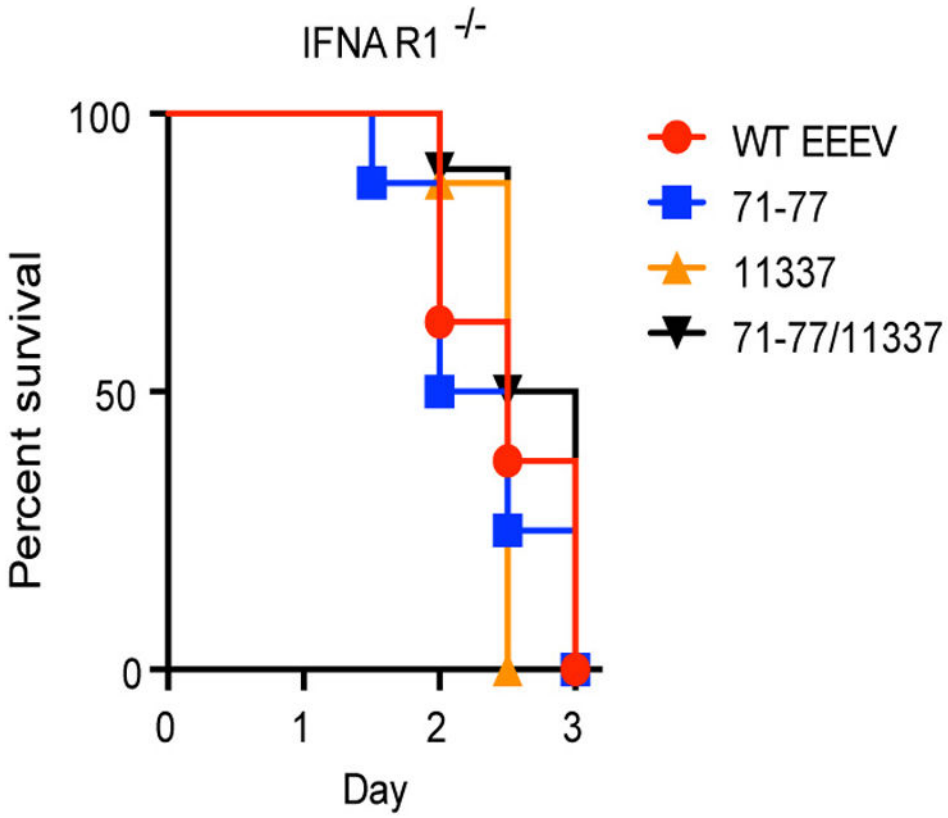

Extended Data Figure 7. Type I IFN attenuates 11337 and 71-77/11337

Survival curves in IFNAR$^{-/-}$ mice. *n* = 8 and 10 (71-77/11337) mice per virus from two independent experiments.

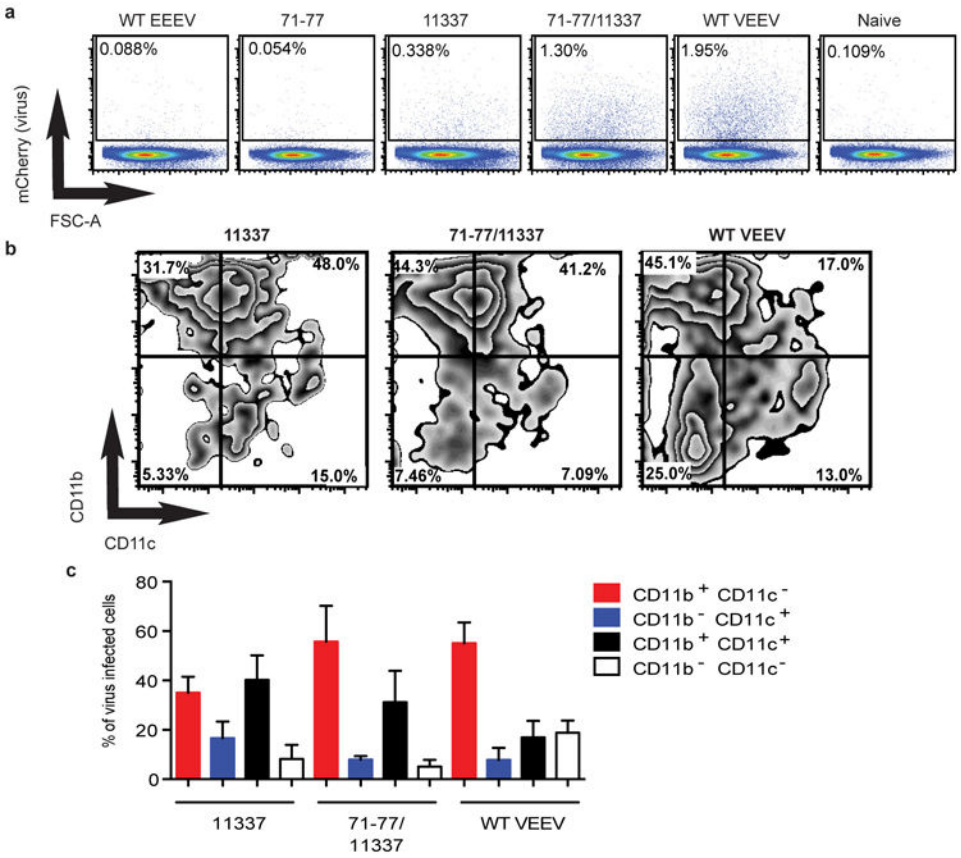

Extended Data Figure 8. EEEV 11337 and 71-77/11337 infect myeloid lineage cells in the PLN

a. Percent virus-infected cells in PLN in naïve, WT VEEV, WT EEEV, 71-77, 11337, and 71-77/11337 infected mice. Plots are representative of *n* = 4 (naïve), 5 (71-77), or 6 mice from two independent experiments. **b-c**. WT VEEV, 11337 and 71-77/11337 infect myeloid lineage cells in the PLN. **b**. Representative flow plot frome 1 mice of CD11b (y-axis) and CD11c (x-axis) expression on virus-infected cells. *n* = 4 (naïve), 5 (71-77) or 6 mice from 2 independent experiments. **c**. Summary of CD11b and CD11c expression on virus-infected cells from WT VEEV, 11337, and 71-77/11337 infected PLNs. Only mice with responses above naïve mice background levels were used to determine CD11b and CD11c expression.

Extended Data Table 1

Primers used to generate the translation reporters using the Quikchange II XL mutagenesis kit

Reporter	Primer Name	Sequence
EEEV Δ5′ NTR	EEEV Δ5′ NTR-F	5′ –agctcggatcctaatacgactcactatagatggagaaagttcatgttgacttagacgca–3′
	EEEV Δ5′ NTR-R	5′ –tgcgtctaagtcaacatgaactttctccatctatagtgagtcgtattaggatccgagct–3′
VEEV Δ5′ NTR	VEEV Δ5′ NTR-F	5′ –agaggatccctaatacgactcactatagatggagaaagttcacgttgacatcgaggaa–3′
	VEEV Δ5′ NTR-R	5′ –ttcctcgatgtcaacgtgaactttctccatctatagtgagtcgtattagggatcctct–3′
Host mimic w/Not1	fLuc-Not1-F	5′ –cccaaaaaaaaaaaaaaaaaaaaaaaaaaaaaaagcggccgccgtaatcatgtcatagc–3′

Reporter	Primer Name	Sequence
	fLuc-Not1-R	5′ –gctatgacatgattacggcggccgctttttttttttttttttttttttttttggg–3′

Extended Data Table 2

Primers used in the generation of EEEV mutant viruses

Virus	Primer Name	Sequence
11337	EEEV11337-F	5′ –gacattaacatcttgtcaaccggcagcgcataatgctgtcttttatatc–3′
	EEEV11337-R	5′ –gatataaaagacagcattatgcgctgccggttgacaagatgttaatgtc–3′
142del	EEEV-Del-1-2-F	5′ –catagacattaacatcttgggcagtgtataaggcttcaccctagttcgatgtacttccg–3′
	EEEV-Del-1-2-R	5′ –cggaagtacatcgaactagggtgaagccttatacactgcccaagatgttaatgtctatg–3′
	EEEV-Del-3-4-F	5′ –ctttataatcaggcataattgggtaatataccgcctggcagcgcataatgctgtc–3′
	EEEV-Del-3-4-R	5′ –gacagcattatgcgctgccaggcggtatattacccaattatgcctgattataaag–3′
142pm	ΔmiR-142-1-F	5′ –taacatcttgtcaaccacataactcaagaggcagtgta–3′
	ΔmiR-142-1-R	5′ –attgtagaacagttggtgtattgagttctccgtcacat–3′
	ΔmiR-142-2-F	5′ –taaggctgtcttactaaactcaagattcaccctag–3′
	ΔmiR-142-2-R	5′ –ctagggtgaatcttgagtttagtaagacagcctta–3′
	ΔmiR-142-3-F	5′ –gcataattgccgtatatacaattactcaagaggtaatataccgcctcttataaa–3′
	ΔmiR-142-3-R	5′ –tttataagaggcggtatattacctcttgagtaattgtatatacggcaattatgc–3′
	ΔmiR-142-4-F	5′ –ataccgcctcttataaactcaagaggcagcgc–3′
	ΔmiR-142-4-R	5′ –gcgctgcctcttgagtttataagaggcggtat–3′

Acknowledgments

We thank Matthew Dunn for excellent technical support, and Michael Diamond for critical reading of the manuscript. This work was supported by National Institute of Heath (NIH) training grant AI049820-10 and AI060525-08 (D.W.T.), research grants AI083383, AI095436 (W.B.K.), and a Project Grant (K.D.R.) from NIAID through the Pacific Northwest Regional Centers for Excellence in Biodefense and Emerging Infectious Diseases Research (PNWRCE; U54 AI081680). The views expressed are those of the authors and do not necessarily represent the views of the NIH.

References

1. Cullen BR. MicroRNAs as mediators of viral evasion of the immune system. Nat Immunol. 2013; 14:205–210. [PubMed: 23416678]
2. Pham AM, Langlois RA, tenOever BR. Replication in cells of hematopoietic origin is necessary for Dengue virus dissemination. PLoS Pathog. 2012; 8:e1002465. [PubMed: 22241991]
3. Zheng Z, et al. Human MicroRNA hsa-miR-296-5p Suppresses Enterovirus 71 Replication by Targeting the Viral Genome. J Virol. 2013; 87:5645–5656. [PubMed: 23468506]
4. Bartel DP. MicroRNAs: Target Recognition and Regulatory Functions. Cell. 2009; 136:215–233. [PubMed: 19167326]
5. Doench JG. Specificity of microRNA target selection in translational repression. Gene Dev. 2004; 18:504–511. [PubMed: 15014042]
6. Djuranovic S, Nahvi A, Green R. miRNA-Mediated Gene Silencing by Translational Repression Followed by mRNA Deadenylation and Decay. Science. 2012; 336:237–240. [PubMed: 22499947]
7. Otsuka M, et al. Hypersusceptibility to Vesicular Stomatitis Virus Infection in Dicer1-Deficient Mice Is Due to Impaired miR24 and miR93 Expression. Immunity. 2007; 27:123–134. [PubMed: 17613256]

8. Lecellier CH. A Cellular MicroRNA Mediates Antiviral Defense in Human Cells. Science. 2005; 308:557–560. [PubMed: 15845854]
9. Shimakami T, et al. Stabilization of hepatitis C virus RNA by an Ago2-miR-122 complex. Proc Natl Acad Sci USA. 2012; 109:941–946. [PubMed: 22215596]
10. Jopling CL. Modulation of Hepatitis C Virus RNA Abundance by a Liver-Specific MicroRNA. Science. 2005; 309:1577–1581. [PubMed: 16141076]
11. Griffin, DE. Alphaviruses. Lippincott Williams & Wilkins; Philadelphia, PA: 2006. p. 1023-1068.
12. Armstrong PM, Andreadis TG. Eastern equine encephalitis virus--old enemy, new threat. N Eng J Med. 2013; 368:1670–1673.
13. Gardner CL, et al. Eastern and Venezuelan Equine Encephalitis Viruses Differ in Their Ability To Infect Dendritic Cells and Macrophages: Impact of Altered Cell Tropism on Pathogenesis. J Virol. 2008; 82:10634–10646. [PubMed: 18768986]
14. Gardner CL, Ebel GD, Ryman KD, Klimstra WB. Heparan sulfate binding by natural eastern equine encephalitis viruses promotes neurovirulence. Proc Natl Acad Sci USA. 2011; 108:16026–16031. [PubMed: 21896745]
15. Silverman MA, et al. Eastern Equine Encephalitis in Children, Massachusetts and New Hampshire, USA, 1970–2010. Emerg Infect Dis. 2013; 19:194–201. [PubMed: 23343480]
16. MacDonald GH, Johnston RE. Role of dendritic cell targeting in Venezuelan equine encephalitis virus pathogenesis. J Virol. 2000; 74:914–922. [PubMed: 10623754]
17. Enright AJ, et al. MicroRNA targets in Drosophila. Genome Biol. 2003; 5:R1. [PubMed: 14709173]
18. Kertesz M, Iovino N, Unnerstall U, Gaul U, Segal E. The role of site accessibility in microRNA target recognition. Nat Genet. 2007; 39:1278–1284. [PubMed: 17893677]
19. Pruitt KD, Tatusova T, Brown GR, Maglott DR. NCBI Reference Sequences (RefSeq): current status, new features and genome annotation policy. Nucleic Acids Res. 2011; 40:D130–D135. [PubMed: 22121212]
20. Mildner A, et al. Mononuclear phagocyte miRNome analysis identifies miR-142 as critical regulator of murine dendritic cell homeostasis. Blood. 2013; 121:1016–1027. [PubMed: 23212522]
21. Lagos-Quintana M, et al. Identification of tissue-specific microRNAs from mouse. Curr Biol. 2002; 12:735–739. [PubMed: 12007417]
22. Bernard KA, Klimstra WB, Johnston RE. Mutations in the E2 Glycoprotein of Venezuelan Equine Encephalitis Virus Confer Heparan Sulfate Interaction, Low Morbidity, and Rapid Clearance from Blood of Mice. Virology. 2000; 276:93–103. [PubMed: 11021998]
23. Langlois RA, Varble A, Chua MA, García-Sastre A, tenOever BR. Hematopoietic-specific targeting of influenza A virus reveals replication requirements for induction of antiviral immune responses. Proc Natl Acad Sci USA. 2012; 109:12117–12122. [PubMed: 22778433]
24. Scott TW, Weaver SC. Eastern equine encephalomyelitis virus: epidemiology and evolution of mosquito transmission. Adv Virus Res. 1989; 37:277–328. [PubMed: 2574935]
25. Tesfay MZ, et al. Alpha/Beta Interferon Inhibits Cap-Dependent Translation of Viral but Not Cellular mRNA by a PKR-Independent Mechanism. J Virol. 2008; 82:2620–2630. [PubMed: 18160435]
26. Bick MJ, et al. Expression of the Zinc-Finger Antiviral Protein Inhibits Alphavirus Replication. J Virol. 2003; 77:11555–11562. [PubMed: 14557641]
27. Anishchenko M, et al. Generation and Characterization of Closely Related Epizootic and Enzootic Infectious cDNA Clones for Studying Interferon Sensitivity and Emergence Mechanisms of Venezuelan Equine Encephalitis Virus. J Virol. 2003; 78:1–8. [PubMed: 14671082]
28. Aguilar PV, et al. Structural and Nonstructural Protein Genome Regions of Eastern Equine Encephalitis Virus Are Determinants of Interferon Sensitivity and Murine Virulence. J Virol. 2008; 82:4920–4930. [PubMed: 18353963]
29. Thomas JM, Klimstra WB, Ryman KD, Heidner HW. Sindbis Virus Vectors Designed To Express a Foreign Protein as a Cleavable Component of the Viral Structural Polyprotein. J Virol. 2003; 77:5598–5606. [PubMed: 12719552]

30. Brault AC, et al. Venezuelan equine encephalitis emergence: enhanced vector infection from a single amino acid substitution in the envelope glycoprotein. Proc Natl Acad Sci USA. 2004; 101:11344–11349. [PubMed: 15277679]

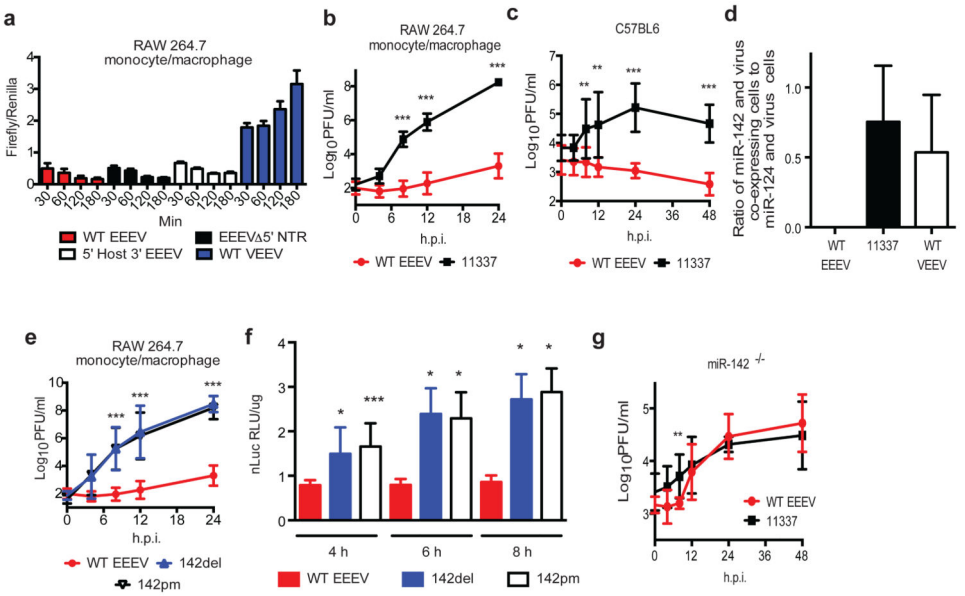

Figure 1. EEEV restriction in myeloid cells is due to miR-142-3p binding sites in the 3′ NTR

a. The EEEV 3′ NTR restricts translation in RAW cells. Errors bars represent mean ± standard deviation (S.D.), from 3 independent experiments. **b-c.** Replication of WT EEEV and 11337 in RAW cells (**b**), and C57BL6BMDCs (**c**). **d.** Overexpression of miR-142-3p in BHK-21 cells blocks EEEV infection compared to overexpression of the control miR-124. Data is represented as the ratio of the percentage of cells co-expressing the microRNA, miR-142, (eGFP) and virus-infected (mCherry) to cells co-expressing miR-124 and virus-infected. Data are averaged (mean ± S.D.) from two independent experiments. **e.** Replication of EEEV 142del and 142pm in RAW cells. **f.** Ablation of the miR-142-3p binding sites in EEEV increases translation in RAW cells. **g.** Replication of WT EEEV and 11337 are similar in miR-142$^{-/-}$ BMDCs. Data represent the geometric mean ± S.D. from three independent experiments unless indicated. Asterisks indicate differences that are statistically significant (*$p < 0.05$, **$p < 0.01$, ***$p < 0.001$).

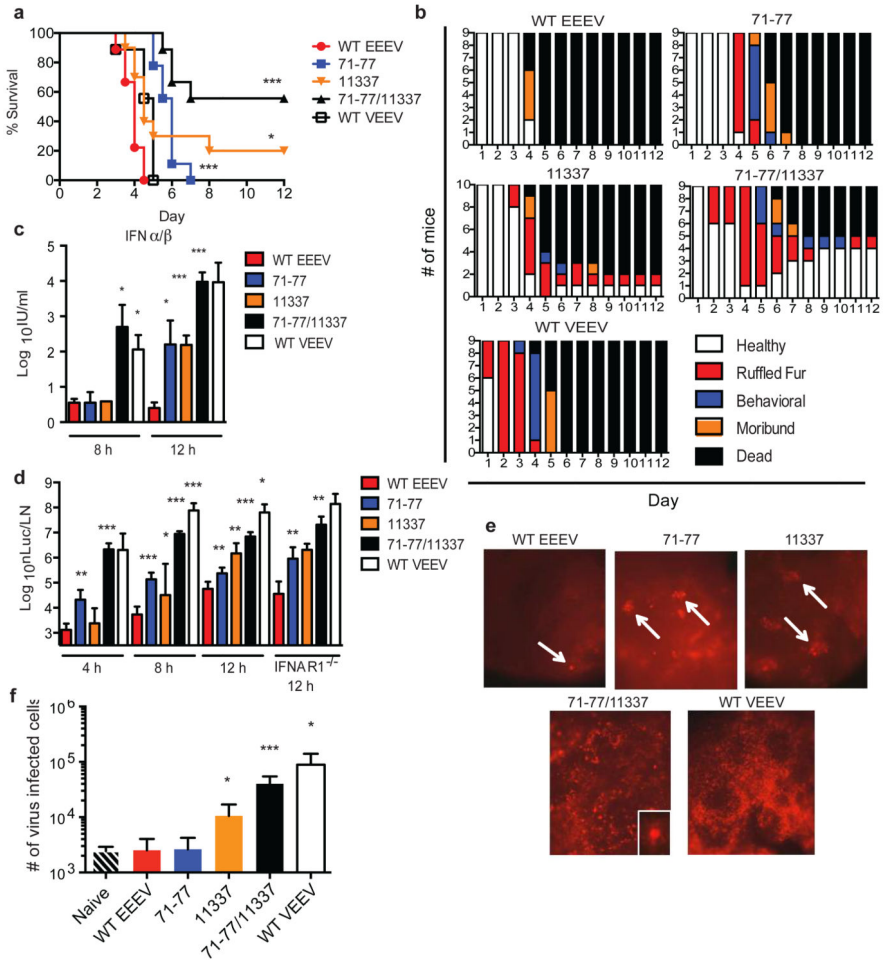

Figure 2. miR-142-3p binding sites in EEEV 3′ NTR decrease virus replication in the lymph node and enhance disease progression

a. Survival curves of CD-1 mice. n = 9 and 10 (11337) mice/group, three independent experiments. **b.** Mice were monitored daily for clinical signs of disease. Y-axis represents number of mice exhibiting each sign of disease on each day. **c.** Serum levels of IFN-α/β in infected CD-1 mice. *n* = 8 mice, two independent experiments. Limit of detection of IFN-α/β ranged from 1.9 IU/ml to 3.9 IU/ml. **d.** Quantification of viral replication in the PLNs using nLuc-reporter viruses. *n* = 8 mice (CD-1) and 6 mice (IFNAR1$^{-/-}$) per time point, two independent experiments. **e.** Visualization of mCherry-reporter virus-infected whole PLN from CD-1 mice 12 h.p.i.. Images are representative of one PLN from two mice. Arrows indicates virus-infected cell(s) in WT EEEV, 71-77, and 11337–infected PLN. **f.** Quantification of virus-infected cells in PLN harvested 12 h.p.i.. *n* = 4 (naïve), 5 (71-77), or 6 mice, two independent experiments. Error bars for all experiments represent geometric mean ± S.D. Asterisks indicate differences for all experiments that are statistically significant (*p < 0.05, **p < 0.01, ***p < 0.001).

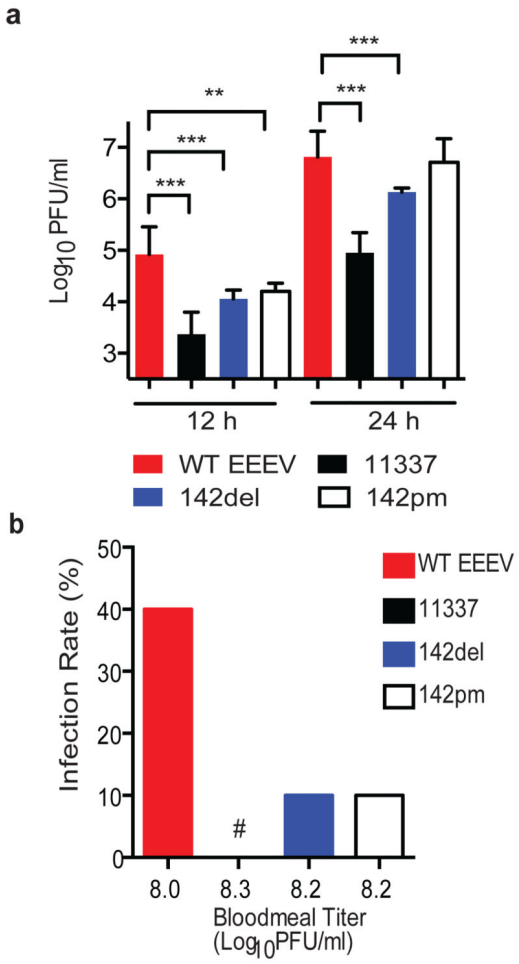

Figure 3. EEEV sequences containing the miR-142-3p binding sites in EEEV are required for efficient mosquito infection

a. Replication of WT EEEV, 11337, 142del and 142pm in C6/36 mosquito cells. *n* = 3 or 4 (11337) independent experiments. Error bars represent geometric mean ± S.D. and asterisks indicate differences that are statistically significant using a two-tailed unpaired t test comparing WT EEEV to all other viruses(** $p < 0.01$, ***$p < 0.001$). **b.** Infection rates of *A. taeniorhynchus* after ingestion of infectious bloodmeals(n = 20 mosquitoes per virus). # Indicates 0 of 20 mosquitoes infected.